Partial magnetic ordering and crystal structure of the ludwigites $Co_2FeO_2BO_3$ and $Ni_2FeO_2BO_3$

D. C. Freitas, M. A. Continentino,* R. B. Guimarães, and J. C. Fernandes
Instituto de Física, Universidade Federal Fluminense, Campus da Praia Vermelha, 24210-340 Niterói, RJ, Brazil

E. P. Oliveira and R. E. Santelli
Departamento de Geoquímica, Universidade Federal Fluminense, Outeiro de S. J. Batista s/n, 24020-150 Niterói, RJ, Brazil

J. Ellena
Instituto de Física de São Carlos, Universidade de São Paulo, Caixa Postal 369, 13560-970 São Carlos, SP, Brazil

G. G. Eslava and L. Ghivelder
Instituto de Física, Universidade Federal do Rio de Janeiro, Caixa Postal 68528, 21945-970 Rio de Janeiro, RJ, Brazil
(Received 13 February 2009; published 30 April 2009)

We present an extensive study of the structural, magnetic, and thermodynamic properties of the two heterometallic oxyborates: $Co_2FeO_2BO_3$ and $Ni_2FeO_2BO_3$. This has been carried out through x-ray diffraction at room temperature (RT) and 150 K, dc and ac magnetic susceptibilities, and specific-heat experiments in single crystals above 2 K. The magnetic properties of these iron *ludwigites* are discussed in comparison with those of the other two known homometallic ludwigites: $Fe_3O_2BO_3$ and $Co_3O_2BO_3$. In both ludwigites now studied we have found that the magnetic ordering of the Fe^{3+} ions occurs at temperatures very near to which they order in $Fe_3O_2BO_3$. A freezing of the divalent ions (Co and Ni) is observed at lower temperatures. Our x-ray diffraction study of both ludwigites at RT and 150 K showed very small ionic disorder in apparent contrast with the freezing of the divalent ion spins. The structural transition that occurs in homometallic $Fe_3O_2BO_3$ has not been found in the present mixed ludwigites in the temperature range investigated.

DOI: 10.1103/PhysRevB.79.134437 PACS number(s): 75.20.Ck, 75.40.−s, 75.30.Kz

I. INTRODUCTION

The ludwigites are oxyborates with general chemical composition $M_2M'O_2BO_3$ where M and M' stand for divalent and trivalent metals, respectively. The known ludwigites containing Fe^{3+} as the trivalent metal have Mg, Fe, Co, Ni, or Cu as divalent metals. The magnetic properties of the first two ludwigites, $Mg_2FeO_2BO_3$ and $Fe_3O_2BO_3$, were extensively studied.[1–8] Also, for $Ni_2FeO_2BO_3$ and $Cu_2FeO_2BO_3$, preliminary studies have been performed.[9,10] However, the magnetic properties of the $Co_2FeO_2BO_3$ ludwigite have never been investigated, to the best of our knowledge.

In the homometallic iron ludwigite, $Fe_3O_2BO_3$, the coexistence of Fe^{3+} magnetic ordering and Fe^{2+} paramagnetism[4,5] has been observed between 70 and 112 K. Also, a subtle structural change, which dimerizes pairs of iron ions along structural subunits in the form of three leg ladders (3LL) occurs in this compound.[6–8] These observations suggested an investigation of the structure and magnetic properties of the *only* other known homometallic ludwigite, $Co_3O_2BO_3$. Surprisingly, a careful study showed that the homometallic cobalt ludwigite does not present any one of the above-mentioned phenomena.[11] We then decided to extend our work to include the ludwigites containing Fe^{3+} ions, such as, $Co_2FeO_2BO_3$ and $Ni_2FeO_2BO_3$. The study of these materials is the subject of the present work. In these compounds, the trivalent ions occupy the sites on the lateral legs of the 3LL's as in both homometallic ludwigites. We have found that these ludwigites behave, in some aspects, similar to the homometallic iron ludwigite: on cooling these systems the Fe^{3+} ions order magnetically while the divalent ions still remain paramagnetic. At lower temperatures however they present a complex behavior. In spite of the absence of positional disorder indicated by the x-ray results, the divalent ions just freeze with no sign for a true thermodynamic magnetic transition. This is shown through magnetic susceptibility and specific-heat experiments performed in these systems above 2 K. $Co_2FeO_2BO_3$ presents a reentrant ferromagnetism, with strong coercivity field, within the temperature range in which Co^{2+} spins freeze. In turn, $Ni_2FeO_2BO_3$ presents only a very weak hysteresis at very low temperatures. Our x-ray diffraction results on single crystals of $Co_2FeO_2BO_3$ and $Ni_2FeO_2BO_3$ at room temperature (RT) and 150 K show that there is no structural phase transition in these compounds. Besides, they give evidence for the absence of any appreciable crystallographic disorder for the occupation of the metallic sites.

II. EXPERIMENTAL

A. Samples preparation

The crystals of both compounds have been synthesized following very similar ways. A 4:1 molar mixture of divalent metal oxide and Fe_2O_3 with an excess of boric acid was fired in borax at 1320 °C for 12 h and slowly cooled down to 600 °C. The borax bath was dissolved in hot water and the crystals washed in diluted cold hydrochloric acid (HCL). Needle shaped black crystals up to 6.5 mm long were obtained for both samples. The good quality of the crystallization was checked through the inspection of the reflection map in three dimensions (3D) of some random chosen dots in the x-ray diffractograms.

One sample of each compound was chemically analyzed

using a *Jobin Yvon Ultima 2* optical emission spectrometry instrument inductively coupled to a plasma source (ICP OES). For data acquisition the ANALYST JY 5.2 software was employed. The analytical wavelengths were 259.940, 228.616, and 221.647 nm for iron, cobalt and nickel, respectively. The solutions for analysis were prepared using analytical grade reagents (*Merck*) and ultrapure water obtained from a reversal osmoses system *Elix and Synergy*, Millipore, Bedford, MA. The samples were prepared by dissolving 0.050 g of each compound in 2 ml of concentrated hydrochloric acid and heated in a water bath at 80 °C until total dissolution of the samples. The obtained results show that there is not a perfect stoichiometry in each compound. For the ludwigite $Co_2FeO_2BO_3$ the found ionic ratio Co/Fe was 2.29 while the ratio Ni/Fe was 2.26 for $Ni_2FeO_2BO_3$ instead of the ideal 2:1 ratio.

B. X-ray diffraction

Prism-shaped crystals were used for data collection from x-ray diffraction. The measurements were carried out on an Enraf-Nonius Kappa-charge-coupled-device (CCD) diffractometer with graphite monochromatic Mo $K\alpha$ radiation (λ =0.710 73 Å). Low temperature measurements were made using an Oxford Cryosystem device. The cell refinements were performed using the software COLLECT (Ref. 12) and SCALEPACK.[13] The final cell parameters were obtained on all reflections. Data were collected up to 62.0° in 2θ. Data reduction was carried out using the software DENZO-SMN, SCALEPACK, and XDISPLAYF (Ref. 13) for visual representation of data. Gaussian absorption correction was applied.[14] The structure was solved using the software SHELXS-97 (Ref. 15) and refined using the software SHELXL-97.[16] All atoms were clearly solved and full-matrix least-squares refinement procedures on F^2 with anisotropic thermal parameters was carried on using SHELXL-97. Crystal data, data collection parameters, and structure refinement data are summarized in Tables I and II. Tables were generated by WINGX.[17] Others software were also used in order to publish the crystal data such as ORTEP-3 (Ref. 18) and DIAMOND 2.1*e* by Bergerhoff *et al.*[19]

We decided to resolve each structure at 293 and 150 K, in analogous experimental conditions, in order to observe any eventual conformational change with temperature as it has been done for homometallic iron ludwigite.[6] No evidence for any phase transition was found.

Figure 1 shows a schematic structure of the $M_2FeO_2BO_3$ ludwigite projected along the *c* axis together with the polyhedra centered at *M* and Fe ions. Figure 2 shows an *Ortep*-type view of the asymmetric unit plus the coordination environment around Co and Fe ions. The bond lengths for $Co_2FeO_2BO_3$ and $Ni_2FeO_2BO_3$ are shown in Tables III and IV, respectively. The mean B-O bond length and the mean O-B-O bond angle are in good agreement with the expected trigonal planar geometry. It is important to note that the coordinations around the M1, M3, and Fe4 sites are distorted octahedra. The coordination bond lengths appear to be more homogeneous around M2. Tables V and VI show the fractional coordinates and the sites occupation factor for each compound.

TABLE I. Crystal data and structure refinement of $Co_2FeO_2BO_3$.

Empirical formula	Co_2FeBO_5	
Formula weight	264.52	
Wavelength	0.717073 Å	
Temperature	293(2) K	150.0 K
Crystal system	Orthorhombic	Orthorhombic
Space group	*Pbam*	*Pbam*
Unit cell dimension *a*=	9.3249(3) Å	9.3149(4) Å
b=	12.2684(6) Å	12.2600(6) Å
c=	3.0308(2) Å	3.03550(10) Å
Volume	347.54(3) Å^3	346.66(3) Å^3
Z	4	4
Density (calculated)	5.055 Mg/m^3	5.068 Mg/m^3
Crystal size (μm^3)	370×94×92	413×159×139
Absorption coefficient	13.442/mm	13.476/mm
F(000)	500	500
θ range (deg.)	2.91 to 32.03	2.91 to 30.508
Index range *h*=	−13, 13	−12, 13
k=	−18, 18	−17, 17
l=	−4, 3	−3, 4
Reflections collected	3664	3451
Independent reflections	708	603
R(int)	0.0581	0.0545
Completeness to θ max	99.7%	96.9%
Absorption correction	Gaussian	Gaussian
Max./min. transmission	0.283/0.639	0.0725/0.2542
Refinement method: Full-matrix least squares on F^2		
data/restraints/parameters	708/0/58	603/0/57
Goodness-of-fit on F^2	1.064	1.079
Final *R* indices [$I>2\sigma(I)$]	$R1=0.0325$	$R1=0.0310$
	$wR2=0.0844$	$wR2=0.0795$
R indices (all data)	$R1=0.0355$	$R1=0.0336$
	$wR2=0.0862$	$wR2=0.0807$
Extinction coefficient	0.03(2)	none
Largest diff. peak	1.90 e Å^{-3}	0.80 e Å^{-3}
Largest diff. hole	−1.32 e Å^{-3}	−1.10 e Å^{-3}

Space groups of $Co_2FeO_2BO_3$ and $Ni_2FeO_2BO_3$ are the same as that found for $Fe_3O_2BO_3$ at RT with comparable cell parameters. Therefore these structures also present 3LL like those found in $Fe_3O_2BO_3$ (Ref. 6), now formed by metal sites Fe4-M2-Fe4. In $Fe_3O_2BO_3$ the central column of these 3LL distorts below 283 K forming zigzag columns along the *c* axis.[6] In $Co_2FeO_2BO_3$ as in $Ni_2FeO_2BO_3$ no distortion appears. The Fe4-M2 bond lengths are 2.8248(5) and 2.7953(7) Å in $Co_2FeO_2BO_3$ and $Ni_2FeO_2BO_3$, respectively. In $Fe_3O_2BO_3$ the corresponding length[6] is 2.786(1) Å.

TABLE II. Crystal data and structure refinement of $Ni_2FeO_2BO_3$.

Empirical formula	Ni_2FeBO_5	
Formula weight	264.08	
Wavelength	0.717073 Å	
Crystal size	$0.284\times0.145\times0.118$ mm^3	
Temperature	293(2) K	150.0 K
Crystal system	orthorhombic	orthorhombic
Space group	*Pbam*	*Pbam*
Unit cell dimension a=	9.2000(9) Å	9.1924(6) Å
b=	12.2261(8) Å	12.2156(9) Å
c=	3.0018(4) Å	2.9982(2) Å
Volume	337.64(6) Å^3	336.62(4) Å^3
Z	4	4
Density (calculated)	5.195 Mg/m^3	5.211 Mg/m^3
Absorption coefficient	15.163/mm	15.209/mm
F(000)	508	508
θ range (degrees)	2.91 to 29.575	3.34 to 26.34
Index range h=	−11, 11	−11, 11
k=	−15, 15	−15, 15
l=	−3, 3	−3, 3
Reflections collected	2216	2199
Independent reflections	439	414
R(int)	0.0566	0.0603
Completeness to θ max	99.1%	99.8%
Absorption correction	Gaussian	Gaussian
Max./min. transmission	0.255/0.086	0.2626/0.1003
Refinement method: Full-matrix least squares on F^2		
data/restraints/parameters	439/0/58	414/0/58
Goodness-of-fit on F^2	1.168	1.106
Final R indices $[I>2\sigma(I)]$	$R1$=0.0282	$R1$=0.0279
	$wR2$=0.0710	$wR2$=0.0727
R indices (all data)	$R1$=0.0285	$R1$=0.0295
	$wR2$=0.0712	$wR2$=0.0740
Extinction coefficient	0.05065	0.04584
Largest diff. peak	1.41 e Å^{-3}	1.09 e Å^{-3}
Largest diff. hole	−1.13 e Å^{-3}	−1.15 e Å^{-3}

C. Magnetic measurements

We have performed a detailed investigation of the magnetic properties of the Co-Fe and Ni-Fe ludwigite systems using a commercial *PPMS platform Quantum Design*. The employed masses were 60.0 and 218.5 mg for $Co_2FeO_2BO_3$ and $Ni_2FeO_2BO_3$, respectively. Figures 3–7 contain the results obtained for $Co_2FeO_2BO_3$ and $Ni_2FeO_2BO_3$. From these figures we have obtained the magnetic parameters found in Table VII except the magnetic ordering temperatures T_C of the Fe^{3+} ions which have been obtained from specific-heat measurements (see Fig. 8). However, the magnetic ordering of the iron ions may also be observed as small

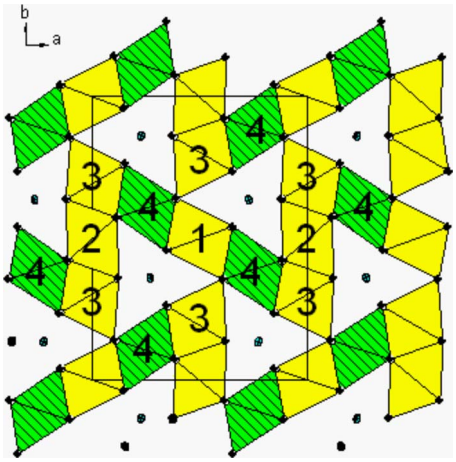

FIG. 1. (Color online) The schematic structure of $M_2FeO_2BO_3$ ludwigites projected along the c axis, together with the oxygen polyhedra centered on the M and Fe^{3+} ions. The lines indicate the a and b axes of the unit cell and the dots the boron ions.

anomalies in the $M\times T$ and $\chi'\times T$ curves of each ludwigite (see Figs. 3 and 4). These temperatures have been shown unambiguously to be the critical ordering temperatures of Fe^{3+} in $Fe_3O_2BO_3$ and $Ni_2FeO_2BO_3$ by means of Mössbauer spectroscopy[4,9] and by neutron scattering in the former system.[8] For $Co_2FeO_2BO_3$ this should also be the case.

The effective magnetic-moment p_{eff} values have been obtained from the high-temperature susceptibilities which are well fitted, as can be seen in the dc magnetization figures, by the equation,

$$\chi = \frac{C}{T-\theta_{\text{CW}}}, \tag{1}$$

where C is related to the *average effective moment* p_{eff} by $C=N(p_{\text{eff}}\mu_B)^2/3k_B$. For that, all the magnetic moments were assumed equal in each compound.

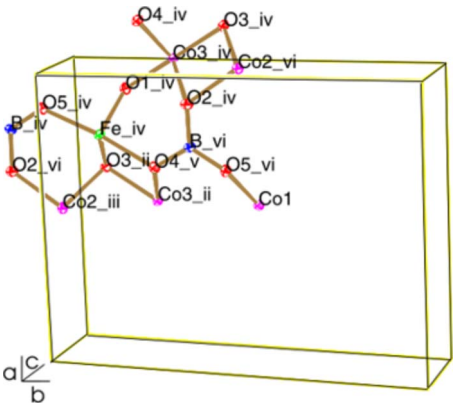

FIG. 2. (Color online) ORTEP-type view of the structure fragment of ludwigite. Ellipsoids are drawn at the 60% probability level. (i) x, y, and z; (ii) $-x$, $-y$, and z; (iii) $x+1/2$, $-y+1/2$, and $-z$; (iv) $-x+1/2$, $y+1/2$, and $-z$; (v) $-x$, $-y$, and $-z$; (vi) x, y, and $-z$; (vii) $-x-1/2$, $y-1/2$, and z ; (viii) $x-1/2$, $-y-1/2$, and z ; (ix) x, y, and $1+z$; and (x) $x-1/2$, $-y+1/2$, and $-z$.

TABLE III. Selected bond lengths in Å for $Co_2FeO_2BO_3$. For symmetry codes see Fig. 2.

Co1-O1	2.023(2)	B-O2^{vii}	1.377(4)
Co1-O5	2.1444(17)	B-O4^{v}	1.396(4)
Co2-O2^{iii}	2.068(2)	Co1-Co1^{ix}	3.0380(2)
Co2-O3^{iii}	2.0876(17)	Co1-Fe4^{ii}	3.0400(5)
Co3-O1	1.950(2)	Co2-Fe4	2.8248(5)
Co3-O3	2.059(3)	Co2-Co2^{ix}	3.0380(2)
Co3-O2^{i}	2.1527(18)	Co2-Co3^{iii}	3.1022(5)
Co3-O4^{i}	2.1568(16)	Co3-Co3^{ix}	3.0380(2)
Fe4-O1	1.9780(17)	Co3-Co1	3.4292(5)
Fe4-O4^{iii}	2.073(2)	Co3-Fe4^{x}	3.1465(6)
Fe4-O5	2.095(2)	Fe4-Fe4^{ix}	3.0380(2)
Fe4-O3^{iii}	2.0977(17)	Fe4-Co3	3.3630(6)
B-O5	1.364(4)		

TABLE IV. Selected bond lengths in Å for $Ni_2FeO_2BO_3$. For symmetry codes see Fig. 2.

Ni1-O1^{iii}	2.011(3)	B-O2	1.390(5)
Ni1-O3	2.1005(19)	B-O3	1.368(5)
Ni2-O4	2.0523(19)	Ni1-Ni1^{ix}	3.0018(4)
Ni2-O5	2.071(3)	Ni1-Fe4	3.0024(6)
Ni3-O1^{iii}	1.942(3)	Ni2-Fe4^{x}	2.7953(7)
Ni3-O4^{vii}	2.059(3)	Ni2-Ni2^{ix}	3.0018(4)
Ni3-O2	2.1114(18)	Ni2-Ni3	3.0654(6)
Ni3-O5^{iii}	2.117(2)	Ni3-Ni3^{ix}	3.0018(4)
Fe4-O1	1.9960(2)	Ni3-Ni1	3.4402(7)
Fe4-O4^{vi}	2.085(2)	Ni3-Fe4^{ix}	3.1120(8)
Fe4-O2	2.076(2)	Fe4-Fe4^{ix}	3.0018(4)
Fe4-O3^{vi}	2.093(3)	Fe4-Ni3	3.3396(8)
B-O5	1.375(5)		

TABLE V. Fractional coordinates and site occupation factor (SOF) for $Co_2FeO_2BO_3$.

Site	x/a	y/b	z/c	SOF
Co(1)	0	0	0	1/4
Co(2)	1/2	0	1/2	1/4
Co(3)	−0.00075(4)	0.27952(4)	0	1/2
Fe(4)	0.23798(5)	0.11555(4)	1/2	1/2
O(1)	0.1072(3)	0.14339(18)	0	1/2
O(2)	0.3762(3)	−0.13986(19)	1/2	1/2
O(3)	−0.1154(3)	0.4230(2)	0	1/2
O(4)	0.1548(2)	−0.2364(2)	1/2	1/2
O(5)	0.1524(3)	−0.0424(2)	1/2	1/2
B	0.2286(4)	−0.1373(3)	1/2	1/2

TABLE VI. Fractional coordinates and site occupation factor (SOF) for $Ni_2FeO_2BO_3$.

Site	x/a	y/b	z/c	SOF
Ni(1)	1/2	0	1/2	1/4
Ni(2)	1/2	1/2	0	1/4
Ni(3)	0.50010(5)	0.28138(4)	1/2	1/2
Fe(4)	0.73757(6)	0.11522(5)	0	1/2
O(1)	0.6059(3)	0.1439(2)	1/2	1/2
O(2)	0.3497(3)	0.2374(2)	0	1/2
O(3)	0.3506(3)	0.0426(2)	0	1/2
O(4)	0.3861(3)	0.4240(2)	1/2	1/2
O(5)	0.6251(3)	0.3592(2)	0	1/2
B	0.2745(5)	0.1387(4)	0	1/2

An important point to be remarked concerning the four ludwigites mentioned in Table VII is that only in the homometallic ludwigites both systems of trivalent and divalent ions fully order magnetically; in spite that $|\theta_{CW}|$ of the heterometallic ludwigites is equivalent or even greater than those of the homometallic ones. In fact, in the last two heterometallic systems of Table VII only the trivalent ions have a magnetic ordering transition at T_C. The remaining magnetic ions just freeze at lower temperatures. This is clearly shown by the specific-heat measurements to be presented in Sec. III. This thermodynamic quantity has distinctive anomalies at the magnetic ordering temperatures of the Fe trivalent ions. At lower temperatures corresponding to the freezing temperatures associated with maxima in the magnetic susceptibility, the specific heat has no distinctive features, similarly to the case of materials exhibiting a spin-glass transition. This is intriguing considering the x-ray results which show that there is no significant crystallographic disorder in these compounds, with the trivalent and divalent ions occupying specific sites in the structure (see Tables V and VI). Specific heat results to be discussed below show clearly an important linear temperature-dependent contribution at low temperatures. Since our samples are nonmetallic, the origin of this

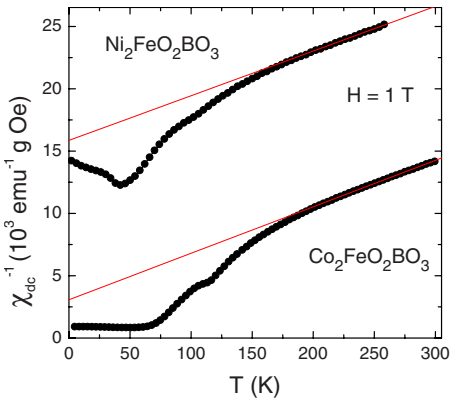

FIG. 3. (Color online) Inverse of dc magnetic susceptibility versus temperature for $Ni_2FeO_2BO_3$ and $Co_2FeO_2BO_3$. The linear fits of the paramagnetic region, $H/M=(1/C)(T-\theta_{CW})$, yield the values of θ_{CW} and of the effective moments p_{eff} given in Table VII.

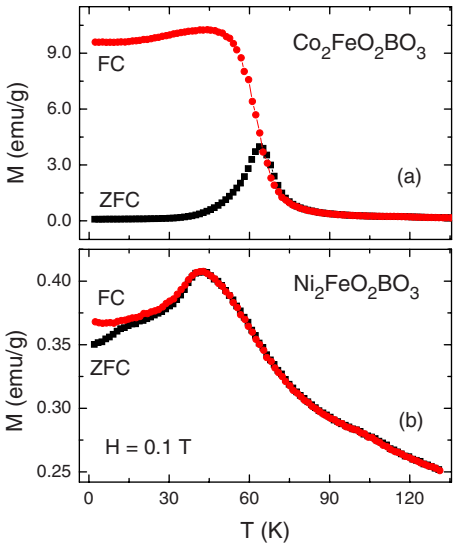

FIG. 4. (Color online) $Co_2FeO_2BO_3$ and $Ni_2FeO_2BO_3$ magnetization versus temperature curves for field cooling and zero-field cooling under an applied magnetic field of 0.1 T.

term is most certainly due to frustration, as usually found in spin-glass systems.

D. Specific-heat measurements

For the purpose of investigating the nature of the magnetic ordering of the Co and Ni ions in the ludwigite structure, we have performed specific-heat measurements in these systems. For $Co_2FeO_2BO_3$ the results were obtained using three crystals of 1.4, 2.1, and 3.3 mg joined together for measuring the specific heat. Only one crystal of 10.2 mg was used for $Ni_2FeO_2BO_3$. The measurements were made using the relaxation technique, in the PPMS platform.

The results are shown in Fig. 8 where in the former, for comparison, we added our previous results for the homometallic ludwigites.[5,11] In the Fe-containing ludwigites one can see clearly features in the specific-heat curves at approximately $T_C \approx 110$ K (the exact values are given in Table VII). These features can be definitely associated with the magnetic ordering of the trivalent Fe ions along the 3LL structures as confirmed by Mössbauer spectroscopy[4,7,9] in $Ni_2FeO_2BO_3$ and in $Fe_2FeO_2BO_3$ and also by neutron scattering[8] in the latter. For the heterometallic systems this is the only thermodynamic magnetic transition, as shown by the specific-heat results. For the homometallic $Fe_3O_2BO_3$ system a second low-temperature feature at T_N=70 K marks the onset of magnetic ordering in the whole system. The ludwigite $Co_3O_2BO_3$ presents only the latter transition.[11] There is no partial ordering in this case. The Néel temperature of this ludwigite, T_N=42 K, obtained from the specific-heat measurements coincides with that obtained from the static and dynamic magnetic measurements.[11] The Néel temperatures (T_N) of the two homometallic ludwigites are not so different

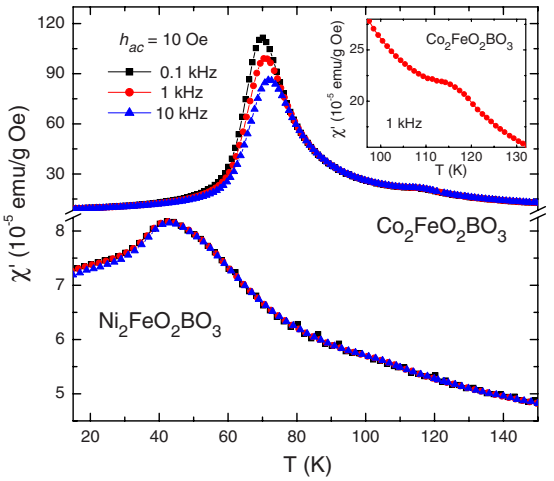

FIG. 5. (Color online) The real part of the ac susceptibilities of $Co_2FeO_2BO_3$ and $Ni_2FeO_2BO_3$ versus temperature at different frequencies. Inset shows an expanded view of the susceptibility of $Co_2FeO_2BO_3$ close to magnetic phase transition.

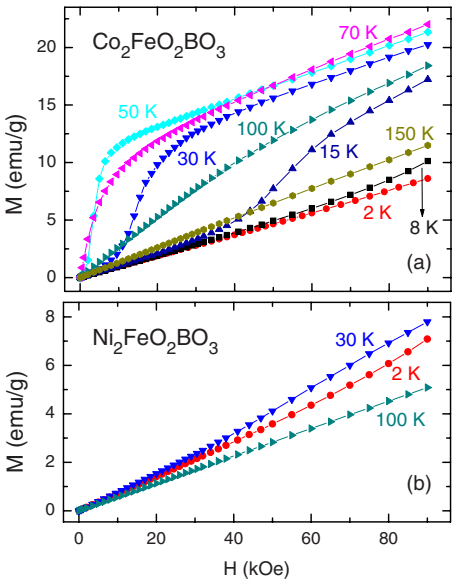

FIG. 6. (Color online) Magnetization versus applied magnetic-field curves for $Co_2FeO_2BO_3$ and $Ni_2FeO_2BO_3$ at several temperatures.

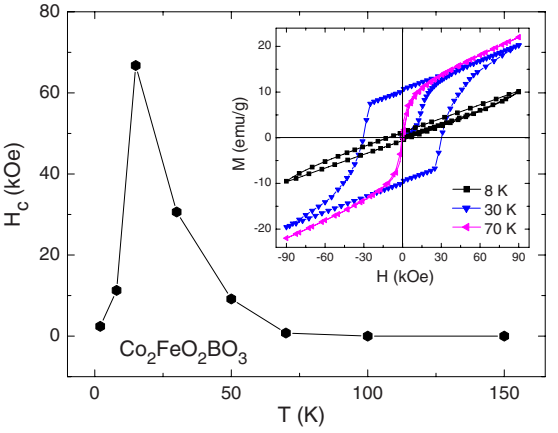

FIG. 7. (Color online) $Co_2FeO_2BO_3$ coercive field values versus temperature. Inset shows hysteresis cycles at different temperatures.

TABLE VII. Magnetic parameters for the ludwigites are discussed in this text. Temperatures are given in Kelvin. θ_{CW} is the Curie-Weiss temperature, T_{C1} is the ordering temperature of the Fe^{3+} ions obtained in the specific-heat measurements, T_{C2} is the ordering temperature of the whole system also obtained in the specific-heat measurements, T_M is the temperature value where the magnetization at 10 kOe maximizes, $T_{\chi'}$ is the same for the real part ac susceptibility at 1 kHz, and p_{eff} is the effective number of Bohr magnetons. pw means present work.

	θ_{CW}	T_{C1}	T_{C2}	T_M	$T_{\chi'}$	p_{eff}	Ref.
$Fe_3O_2BO_3$	−485	112	70	≈70	70	6.6	4 and 6
$Co_3O_2BO_3$	−25		42	<20	42	4.16	11
$Co_2FeO_2BO_3$	−82	117		54	70	4.35	pw
$Ni_2FeO_2BO_3$	−442	105		42	42	4.43	pw

as should be expected from their very different Curie-Weiss temperatures (see Table VII). Since the high-temperature magnetic measurements provide some average of the magnetic interactions, this can be interpreted as due to a predominance of *ferromagnetic interactions* in the Co ludwigite.[11]

The specific-heat measurements confirm our conclusions in Sec. I, that the low-temperature features observed in the magnetic behavior of the heterometallic compounds correspond to a freezing of the magnetic moments of the divalent ions. They are not associated with a true thermodynamic magnetic transition, as they have no corresponding features in the specific-heat measurements.

At the lowest-measured temperatures, the specific heat of our samples exhibit temperature dependencies which are described by power laws being well fitted by the expression, $C/T=\gamma+\beta T^2$, as shown in Fig. 9. The T^3 term in solids is generally due to lattice excitations. In magnetic solids as antiferromagnetic or ferrimagnetic materials, it can also arise

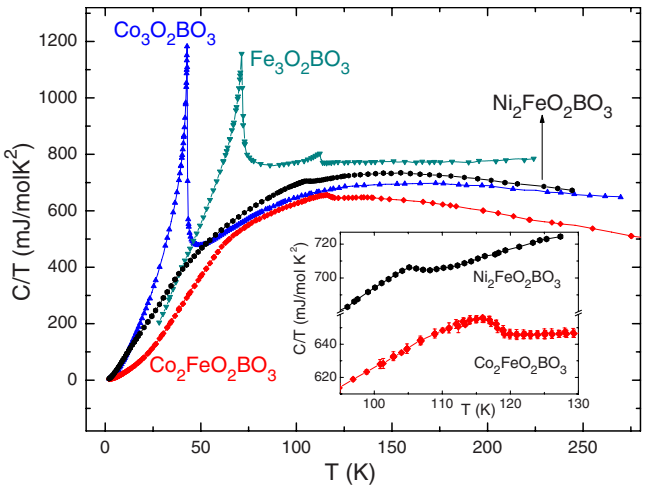

FIG. 8. (Color online) Specific-heat measurements, plotted as $C/T\times T$, for $Fe_3O_2BO_3$, $Co_3O_2BO_3$, $Co_2FeO_2BO_3$, and $Ni_2FeO_2BO_3$. For the homometallic ludwigites the data are taken respectively from Refs. 6 and 11. Inset shows segments of specific-heat curves with error bars. These curves show more clearly the peaks associated with the Fe^{3+} ions ordering.

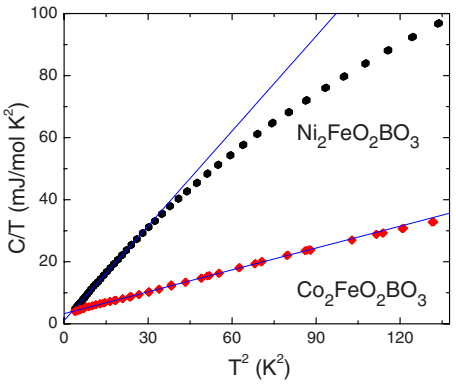

FIG. 9. (Color online) Specific heat measurements plotted as $C/T\times T^2$. The parameters for the linear fit of the low-temperature extremity, $(C/T)=\gamma+\beta T^2$, are $\gamma=1.041$ and $\beta=1.019$ for $Co_2FeO_2BO_3$ and $\gamma=3.282$ and $\beta=0.235$ for $Ni_2FeO_2BO_3$. The units are $mJ/molK^2$ and $mJ/molK^4$, respectively.

from spin waves with a linear dispersion relation. The origin of this contribution has been clarified by comparing the specific-heat results in $H=0$ and $H=9$ T for $Co_3O_2BO_3$ and turns out to be due to lattice excitations[11] associated with a Debye temperature, $\theta_D\approx 140$ K in this material.

The thermodynamic experiments show the existence of a large low-temperature linear dependent contribution for the specific heat of our materials. This contribution is of the order of those found in metallic systems where it is due to conduction electrons. However transport measurements by Ivanova *et al.*[20] in $Co_3O_2BO_3$ in a temperature range well above the magnetic transition and also[4] in $Fe_3O_2BO_3$ have shown a thermally activated behavior of the conductivity which implies the nonmetallic nature of these systems. In insulating materials such linear temperature-dependent term in the specific heat is generally attributed to frustration or disorder. It is surprising anyway that this term is of the same order of magnitude in all ludwigites where they have been measured (see Table VIII), including the Co homometallic system where no disorder is expected and no magnetic freezing but, a true magnetic transition is observed.

III. DISCUSSION

Oxyborates of the ludwigite type present interesting properties related to the interplay of magnetism, structural instabilities, and low dimensionality. A manifestation of this in-

TABLE VIII. The γ and β parameters for the linear fit of the $C/T\times T^2$ plot of the specific-heat measurements. The temperature range for the plotting may be seen in Figs. 8 and 9. pw means present work.

	γ ($mJ/molK^2$)	β ($mJ/molK^2$)	Ref.
$Co_3O_2BO_3$	3.30	0.72	11
$Co_2FeO_2BO_3$	3.28	0.23	pw
$Ni_2FeO_2BO_3$	1.04	1.02	pw

terplay is the existence of a dimerization instability in the 3LL of the Fe ludwigite. Surprisingly, the present study provides continuing evidence that this structural transition is unique to the Fe homometallic system. It was found neither in the Co homometallic ludwigite[11] nor in those investigated here. In all Fe containing ludwigites investigated, Fe^{3+} ions occupy the outer legs of the 3LL. This is one of the sites involved in the dimerization process. The other is the site in the second leg, which only in the homometallic case is also occupied by Fe ions. In $Co_3O_2BO_3$, in spite of the fact that all the elements in the 3LL are Co ions, no dimerization appears. The Fe system is unique also in that it presents two thermodynamic magnetic transitions: a partial magnetic ordering of the ions in the 3LL and, at lower temperatures, the ordering of the whole system. This partial ordering[4] occurs in the dimerized ladders below the structural transition[6] which starts at 283 K. In the $Co_3O_2BO_3$ only the low-temperature transition exists and there is no partial ordering of the moments, as well as, no dimerization.

We have shown here, using x-ray scattering, that in the heterometallic systems the divalent and trivalent ions are found to occupy specific sites in the structure. In particular, Fe^{3+} ions occupy the outer legs along the 3LL as in the homometallic iron ludwigite. In the heterometallic ludwigites the present specific-heat results show that there is a single thermodynamic magnetic transition, which is associated with the ordering of the Fe^{3+} ions in the outer legs of the 3LL. The remaining magnetic ions *freeze* at lower temperatures, as shown by maxima in the magnetic susceptibilities. That this is a freezing phenomenon is shown by the absence of any feature in the specific heat at the freezing temperatures. The magnetic arrangements at low temperatures are complex as can be seen in Figs. 6 and 7 for the Fe-Co system where a clear reentrant behavior is observed.

The contrasting magnetic behavior of the pure and mixed ludwigites, specifically the magnetic freezing in the latter, seems to point for the influence of disorder or frustration. Most probably it is frustration since the x-ray studies give no evidence for crystallographic disorder. Frustration is most certainly present in these materials due to many paths along which antiferromagnetic superexchange interactions may arise. Furthermore, it can produce large effects in the low dimensional ribbons which join to form the ludwigite structure. Independent evidence for frustration in our samples comes from specific-heat measurements that show the presence of a significant linear temperature-dependent term at low temperatures. Since these ludwigites are nonmetallic, this term can be attributed to frustration as observed, for example, in spin glasses. On the other hand, this contribution is also present in the homometallic Co system (see Table VIII) which also shows a single magnetic transition and of course in this case has no substitutional disorder.

It is plausible then that in the Fe system the dimerization transition has a purely electronic origin, i.e., it is a Peierls instability as suggested in Ref. 21. In this case the partial magnetic ordering at lower temperatures arises as a *consequence* of the dimerization and not vice versa.[22] In any case the connection between elastic and magnetic properties in the ludwigites is far from simple and straightforward. Clearly an understanding of the differences in physical behavior of these ludwigites can throw light on the nature of the several competing mechanisms which determine the physical properties of mixed-valence materials, specially in low dimensions.

ACKNOWLEDGMENT

Support from the Brazilian agencies CNPq and FAPERJ is gratefully acknowledged.

*mucio@if.uff.br

[1] A. Wiedenmann, P. Burlet, and R. Chevalier, J. Magn. Magn. Mater. **15-18**, 216 (1980).
[2] H. Neuendorf and W. Gunsser, J. Magn. Magn. Mater. **173**, 117 (1997).
[3] J. Paul Attfield, John F. Clarke, and David A. Perkins, Physica B **180-181**, 581 (1992).
[4] R. B. Guimaraes, M. Mir, J. C. Fernandes, M. A. Continentino, H. A. Borges, G. Cernicchiaro, M. B. Fontes, D. R. S. Candela, and E. Baggio-Saitovich, Phys. Rev. B **60**, 6617 (1999).
[5] J. C. Fernandes, R. B. Guimarães, M. A. Continentino, L. Ghivelder, and R. S. Freitas, Phys. Rev. B **61**, R850 (2000).
[6] M. Mir, R. B. Guimarães, J. C. Fernandes, M. A. Continentino, A. C. Doriguetto, Y. P. Mascarenhas, J. Ellena, E. E. Castellano, R. S. Freitas, and L. Ghivelder, Phys. Rev. Lett. **87**, 147201 (2001); A. P. Douvalis, A. Moukarika, T. Bakas, G. Kallias, and V. Papaefthymiou, J. Phys.: Condens. Matter **14**, 3303 (2002).
[7] J. Larrea J., D. R. Sánchez, F. J. Litterst, E. M. Baggio-Saitovitch, J. C. Fernandes, R. B. Guimarães, and M. A. Continentino, Phys. Rev. B **70**, 174452 (2004).
[8] P. Bordet, E. Suard, J. Dumas, M. Avignon, J.-L. Tholence, M. A. Continentino, and M. Mir, Proceedings of the IUCr XX, Florence, 2005 [Acta Crystallogr., Sect. A: Found. Crystallogr. 61, C57 (2005)].
[9] J. C. Fernandes, R. B. Guimarães, M. A. Continentino, H. A. Borges, A. Sulpice, J.-L. Tholence, J. L. Siqueira, L. I. Zawislak, J. B. M. da Cunha, and C. A. dos Santos, Phys. Rev. B **58**, 287 (1998).
[10] M. A. Continentino, J. C. Fernandes, R. B. Guimarães, H. A. Borges, J.-L. Tholence, J. L. Siqueira, J. B. M. da Cunha, and C. A. dos Santos, Eur. Phys. J. B **9**, 613 (1999).
[11] D. C. Freitas, M. A. Continentino, R. B. Guimarães, J. C. Fernandes, J. Ellena, and L. Ghivelder, Phys. Rev. B **77**, 184422 (2008).
[12] Enraf-Nonius COLLECT (Nonius BV, Delft, The Netherlands, 1997–2000).
[13] Z. Otwinowski and W. Minor, in *Methods in Enzymology*, edited by C. W. Carter, Jr. and R. M. Sweet (Academic, New York, 1997), Vol. 276.
[14] P. Coppens, L. Leiserowitz, and D. Rabinovich, Acta Crystallogr. **18**, 1035 (1965).
[15] SHELXS97—Program for Crystal Structure Solution (Release

97–2) (Sheldrick, G.M., Institüt für Anorganische Chemie der Universität, Tammanstrasse 4, D-3400 Göttingen, Germany, 1998).
[16] SHELXL97—Program for Crystal Structure Refinement (Release 97–2) (Sheldrick, G.M., Institüt für Anorganische Chemie der Universität, Tammanstrasse 4, D-3400 Göttingen, Germany, 1998).
[17] L. J. Farrugia, J. Appl. Crystallogr. **32**, 837 (1999).
[18] L. J. Farrugia, J. Appl. Crystallogr. **30**, 565 (1997).
[19] G. Bergherhoff, M. Berndt, and K. Brandenburg, J. Res. Natl. Inst. Stand. Technol. **101**, 221 (1996).
[20] N. B. Ivanova, A. D. Vasiliév, D. A. Velikanov, N. V. Kazak, S. G. Ovchinnikov, G. A. Petrakovskii, and V. V. Rudenko, Phys. Solid State **49**, 651 (2007).
[21] A. Latge and M. A. Continentino, Phys. Rev. B **66**, 094113 (2002).
[22] E. Vallejo and M. Avignon, Phys. Rev. Lett. **97**, 217203 (2006).